FLAME DETECTION SYSTEM BASED ON WAVELET ANALYSIS OF PIR SENSOR SIGNALS WITH AN HMM DECISION MECHANISM

B. Uğur Töreyin, E. Birey Soyer, Onay Urfalıoğlu, and A. Enis Çetin

Department of Electrical and Electronics Engineering, Bilkent University
06800 Bilkent, Ankara, Turkey
phone: + (90) 312 290 1286, fax: + (90) 312 266 4192, email: {ugur, birey, onay, enis}@ee.bilkent.edu.tr

ABSTRACT

In this paper, a flame detection system based on a pyroelectric (or passive) infrared (PIR) sensor is described. The flame detection system can be used for fire detection in large rooms. The flame flicker process of an uncontrolled fire and ordinary activity of human beings and other objects are modeled using a set of Hidden Markov Models (HMM), which are trained using the wavelet transform of the PIR sensor signal. Whenever there is an activity within the viewing range of the PIR sensor system, the sensor signal is analyzed in the wavelet domain and the wavelet signals are fed to a set of HMMs. A fire or no fire decision is made according to the HMM producing the highest probability.

1. INTRODUCTION

Conventional point smoke and fire detectors typically detect the presence of certain particles generated by smoke and fire by ionization or photometry. An important weakness of point detectors is that the smoke has to reach the sensor. This may take significant amount of time to produce an alarm and therefore it is not possible to use them in open spaces or large rooms. The main advantage of Passive Infrared Sensors (PIR) (or Pyroelectric Infra Red) based sensor system for fire detection over the conventional smoke detectors is the ability to monitor large rooms and spaces because they analyze the infrared light reflected from hot objects or fire flames to reach a decision.

It is reported that turbulent flames of an uncontrolled fire flicker with a frequency of around 10Hz [1, 2]. Recently developed video based fire detection schemes also take advantage of this fact by detecting periodic high-frequency behavior in flame colored moving pixels [3] - [5]. Actually, instantaneous flame flicker frequency is not constant and it varies in time. Flame flicker behaviour is a wide-band activity covering 1 Hz to 13 Hz. Therefore, a Markov model based modeling of flame flicker process produces more robust performance compared to frequency domain based methods. Markov models are extensively used in speech recognition systems and in computer vision applications [6] - [9]. In [14], several experiments on the relationship between burner size and flame flicker frequency are presented. Recent research on pyro-IR based combustion monitoring includes [15] where monitoring system using an array of PIR detectors is realized.

A regular camera or typical IR flame sensors have a fire detection range of 30 meters. The detection range of a PIR sensor based system is 5 meters but this is enough to cover most rooms with high ceilings. Therefore, PIR based systems provide a cost-effective solution to the fire detection problem in relatively large rooms as the unit cost of a camera based system or a regular IR sensor based system is in the order of one thousand dollars.

In this approach, wavelet domain signal processing is used which provides robustness against sensor signal drift due to temperature variations in the observed area. Regular temperature changes are slow variations compared to the moving objects and flames. Since wavelet signals are high-pass and band-pass signals they do not get affected by the slow variations.

There are two different classes of events defined in this approach. The first class represents fire events whereas the second class represents non-fire events. The main application of PIR sensors is hot body motion detection. Therefore, we include regular human motion events like walking or running in the non-fire event class.

In Section 2, we will present the circuit diagram of a typical PIR sensor system and how it is modified for flame detection. In Section 3, the wavelet domain signal processing and the HMM based modeling of the flames and human motion are described. In Section 4, simulation results are presented.

2. PIR SENSOR SYSTEM AND DATA ACQUISITION

Commercially available PIR sensor read-out circuits produce binary outputs. However, it is possible to capture a continuous time analog signal indicating the strength of the received signal in time. The corresponding circuit for capturing an analog signal output is shown in Fig 1.

The circuit consists of 4 operational amplifiers (op amps), IC1A, IC1B, IC1C and IC1D. IC1A and B constitute a two stage amplifier circuit whereas IC1C and D couple behaves as a comparator. The very-low amplitude raw output at the 2nd pin of the PIR sensor is amplified through the two stage amplifier circuit. The amplified signal at the output of IC1B is fed into the comparator structure which outputs a binary signal, either 0 V or 5 V. Instead of using binary output in the original version of the PIR sensor read-out circuit, we directly measure the analog output signal at the output of the 2nd op amp, IC1B.

In order to capture the flame flicker process the analog signal is sampled with a sampling frequency of $f_s = 50Hz$ because the highest flame flicker frequency is 13Hz [2] and $f_s = 50Hz$ is well above $2 \times 13Hz$. In Figure 2, a frequency distribution plot corresponding to a flickering flame of an uncontrolled fire is shown. It is clear that the sampling frequency of 50Hz is sufficient. Typical sampled signal for no activity case using 8 bit quantization is shown in Fig 3. Other typical received signals from a moving person and flickering fire are presented in Fig. 4.

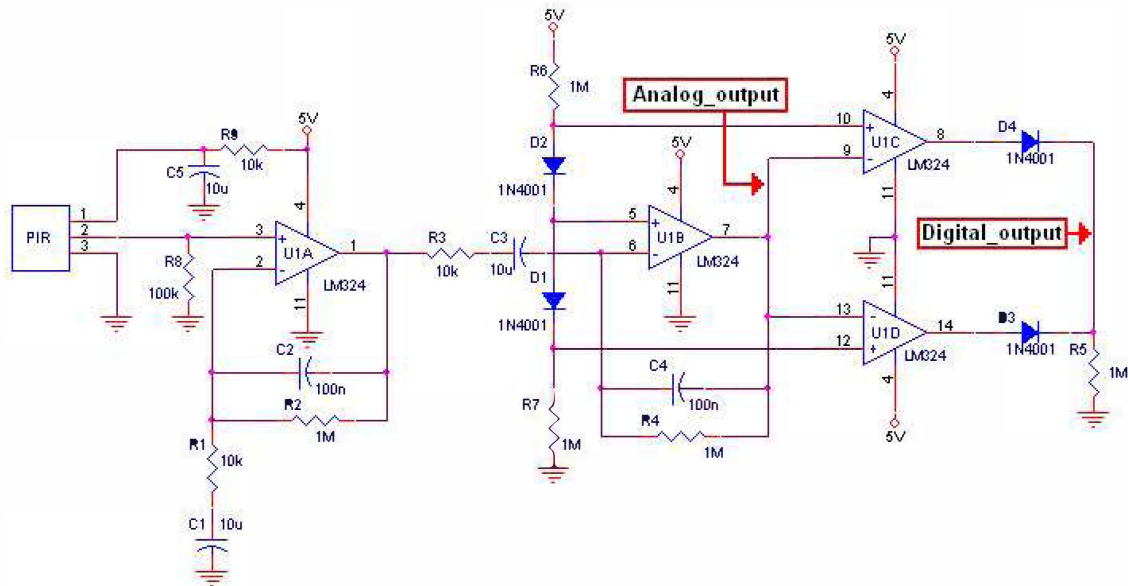The strength of the received signal from a PIR sensor in-

Figure 1: The circuit diagram for capturing an analog signal output from a PIR sensor.

creases when there is motion due to a hot body within its viewing range. In fact, this is due to the fact that pyroelectric sensors give an electric response to a rate of change of temperature rather than temperature itself. On the other hand, the motion may be due to human motion taking place in front of the sensors or flickering flame. In this paper the PIR sensor data is used to distinguish the flame flicker from the motion of a human being like running or walking. Typically the PIR signal frequency of oscillation for a flickering flame is higher than that of PIR signals caused by a moving hot body. In order to keep the computational cost of the detection mechanism low, we decided to use Lagrange filters for obtaining the wavelet transform coefficients as features instead of using a direct frequency approach, such as FFT based methods.

3. SENSOR DATA PROCESSING AND HMMS

There is a bias in the PIR sensor output signal which changes according to the room temperature. Wavelet transform of the PIR signal removes this bias. Let x[n] be a sampled version of the signal coming out of a PIR sensor. Wavelet coefficients obtained after a single stage subband decomposition, w[k], corresponding to [12.5 Hz, 25 Hz] frequency band information of the original sensor output signal x[n] are evaluated with an integer arithmetic high-pass filter corresponding to Lagrange wavelets [13] followed by decimation. The filter bank of a biorthogonal wavelet transform is used in the analysis. The lowpass filter has the transfer function:

$$H_l(z) = \frac{1}{2} + \frac{1}{4}(z^{-1} + z^1) \tag{1}$$

and the corresponding high-pass filter has the transfer function

$$H_h(z) = \frac{1}{2} - \frac{1}{4}(z^{-1} + z^1) \tag{2}$$

An HMM based classification is carried out for fire detection. Two three-state Markov models are used to represent

fire and non-fire events (cf. Fig. 5). In these Markov models, state $S1$ corresponds to no activity within the viewing range of the PIR sensor. The system remains in state $S1$ as long as there is not any significant activity, which means that the absolute value of the current wavelet coefficient, $|w[k]|$, is below a non-negative threshold $T1$. A second threshold $T2$ is also defined in wavelet domain which determines the state transitions between $S2$ and $S3$. If $T1 < |w[k]| < T2$, then state $S2$ is attained. In case of $|w[k]| > T2$, state $S3$ is acquired.

The first step of the HMM based analysis consists of dividing the wavelet coefficient sequences in windows of 25 samples. For each window, a corresponding state transition sequence is determined. An example state transition sequence of size 5 may look like

$$C = (S2, S1, S3, S2, S1) \tag{3}$$

Since the wavelet signal captures the high frequency information in the signal, we expect that there will be more transitions occurring between states when monitoring fire compared to human motion.

3.1 Estimation of thresholds T1 and T2 for state transitions

The thresholds $T1$ and $T2$ in the wavelet domain determine the state transition probabilities, given a signal. In the training step, the task is to find optimal values for $T1$ and $T2$. Given $(T1, T2)$ and ground-truth fire and non-fire wavelet training sequences, it is possible to calculate the transition probabilities for each class. Let a_{ij} denote the transition probabilities for the 'fire' class and b_{ij} denote the transition probabilities for the 'non-fire' class.

The decision about the class affiliation of a state transition sequence C of size L is done by calculating the two joint probabilities $P_a(C)$ and $P_b(C)$ corresponding to fire and non-

fire classes, respectively:

$$P_a(C) = \prod_i p_a(C_{i+1}|C_i) = \prod_i a_{C_i,C_{i+1}} \qquad (4)$$

and

$$P_b(C) = \prod_i p_b(C_{i+1}|C_i) = \prod_i b_{C_i,C_{i+1}} \qquad (5)$$

where $p_a(C_{i+1}|C_i) = a_{C_i,C_{i+1}}$, and $p_b(C_{i+1}|C_i) = \prod_i b_{C_i,C_{i+1}}$, and $i = 1,...,L$.

In case of $P_a(C) > P_b(C)$ the class affiliation of state transition sequence C will be declared as 'fire', otherwise it is declared as 'non-fire'.

Given N_a training sequences $A_1,...,A_{N_a}$ from 'fire' class and N_b training sequences $B_1,...,B_{N_b}$ from 'non-fire' class, the task of the training step is to find the tuple (T1, T2) which maximizes the dissimilarity $D = (S_a - S_b)^2$, where $S_a = \sum_i P_a(B_i)$ and $S_b = \sum_i P_b(A_i)$.

This means, for each given tuple $(T1,T2)$, there is a specific value of the dissimilarity D, so that D is a function of $(T1,T2)$

$$D = D(T1,T2) \qquad (6)$$

Figure 6 shows a typical plot of the dissimilarity function $D(T1,T2)$. It can be seen from this figure that D is multi-modal and and non-differentiable. Therefore, we solve this maximization problem using a Genetic Algorithm (GA) having the objective function $D(T1,T2)$.
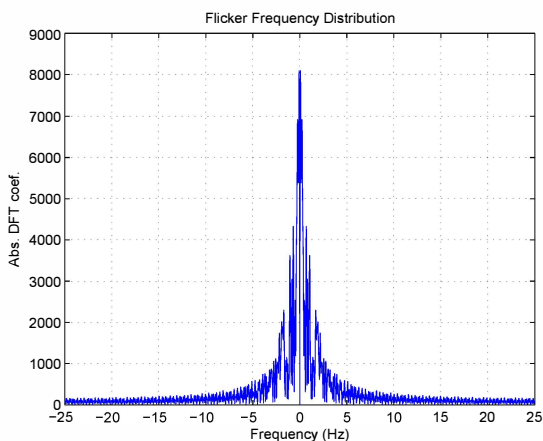

Figure 2: Flame flicker spectrum distribution. PIR signal is sampled with 50 Hz.

For the training of the HMMs, the state transition probabilities for human motion and flame are estimated from 250 consecutive wavelet coefficients covering a time frame of 10 seconds.

During the classification phase a state history signal consisting of 50 consecutive wavelet coefficients are computed from the received sensor signal. This state sequence is fed to fire and non-fire models in running windows. The model yielding highest probability is determined as the result of the analysis of PIR sensor data.

For flame sequences, the transition probabilities $a's$ should be high and close to each other due to random nature of uncontrolled fire. On the other hand, transition probabilities should be small in constant temperature moving bodies like a walking person because there is no change or little
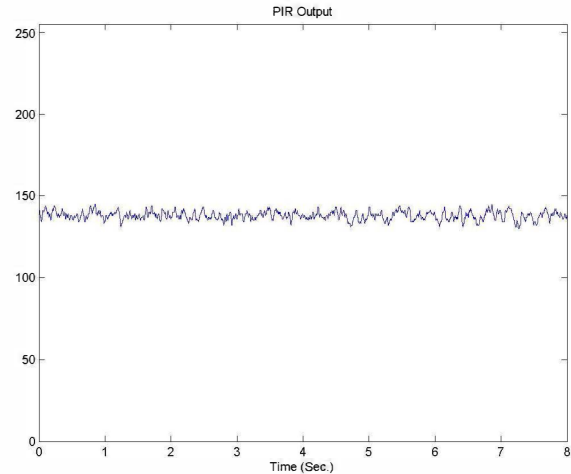

Figure 3: A typical PIR sensor output sampled at 50 Hz with 8 bit quantization when there is no activity within its viewing range.

change in pixel values. Hence we expect a higher probability for b_{00} than any other b value in the non-fire model which corresponds to higher probability of being in $S1$. The state $S2$ provides hysteresis and it prevents sudden transitions from $S1$ to $S3$ or vice versa.

4. EXPERIMENTAL RESULTS

The analog output signal is sampled with a sampling frequency of 50 Hz and quantized at 8 bits. Real-time analysis and classification methods are implemented with C++ running on a PC. Digitized output signal is fed to the PC via RS-232 serial port.

In our experiments we record fire and non-fire sequences at a distance of 5m to the sensor. For fire sequences, we burn paper and alcohol, and record the output signals. For the non-fire sequences, we record walking and running person sequences. The person within the viewing range of the PIR sensor walks or runs on a straight line which is tangent to the circle with a radius of 5m and the sensor being at the center.

The training set consists of 90 fire and 90 non-fire recordings with durations varying between three to four seconds. The test set for fire class is 198 and that of non-fire set is 558. Our method successfully detects fire for 195 of the sequences in the fire test set. It does not trigger fire alarm for any of the sequences in the non-fire test set. This is presented in Table-1.

The false negative alarms, 3 out of 198 fire test sequences, are issued for the recordings where a man was also within the viewing range of the sensor along with a fire close to diminish inside a waste-bin. The test setting for which false alarms are issued is presented in Fig. 7.

5. CONCLUSION

In this paper, a method for flame detection using PIR sensors is proposed. Analog signal from a PIR sensor is sampled with a sampling frequency of 50 Hz and quantized with 8 bits. Single level wavelet coefficients of the output signal are

Table 1: Results with 198 fire, 588 non-fire test sequences. The system triggers an alarm when fire is detected within the viewing range of the PIR sensor.

	Number of Sequences	Number of False Alarms	Number of Alarms
Fire Test Sequences	198	3	195
Non-Fire Test Sequences	588	0	0
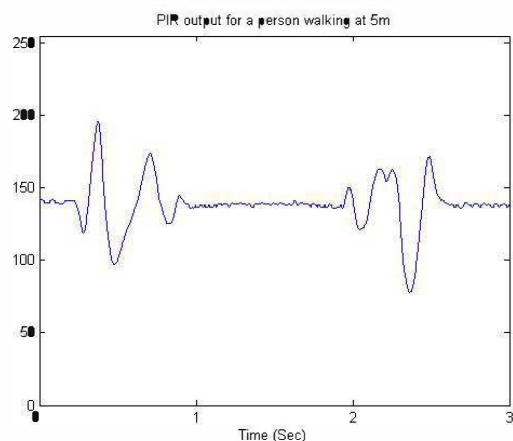
(a) person
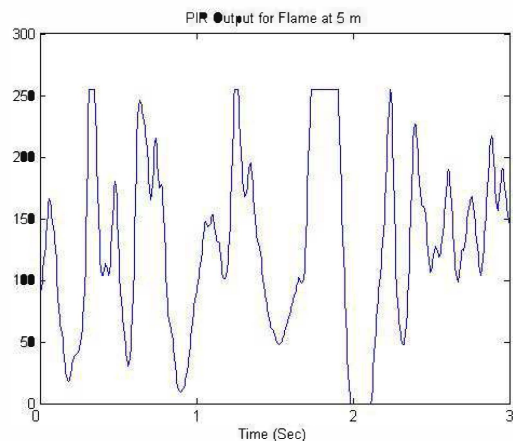
(b) flame

Figure 4: PIR sensor output signals recorded at a distance 5m for a (a) walking person, and (b) flame.
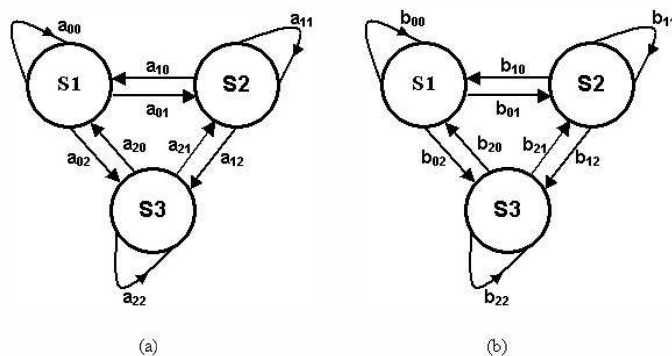

Figure 5: Two three-state Markov models are used to represent (a) 'fire' and (b) 'non-fire' classes, respectively.
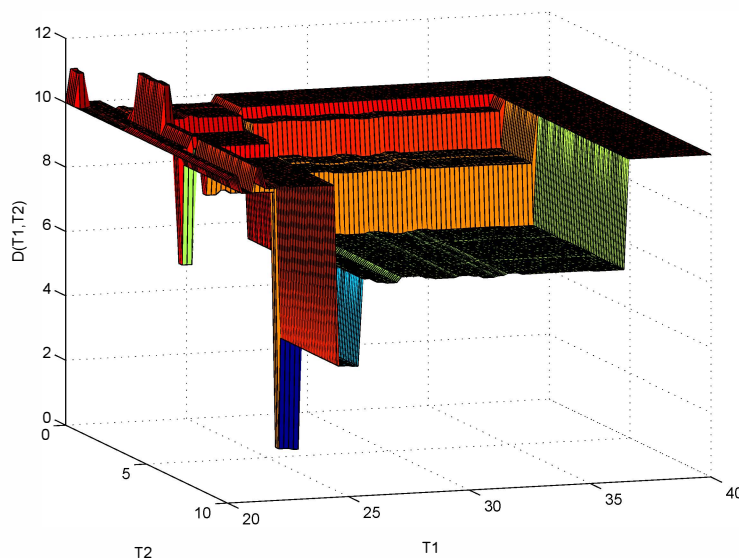

Figure 6: A typical plot of the dissimilarity function $D(T1,T2)x10^{-4}$. It is multi-modal and non-differentiable.

Figure 7: The PIR sensor is encircled. The fire is close to die out completely. A man is also within the viewing range of the sensor.

used as feature vectors for flame detection. PIR sensor output recordings containing various human motions and flames of paper and alcohol fire at a range of 5m are used for training the HMMs corresponding to different events. Thresholds for defining the states of HMMs are estimated using an evolutionary algorithm, since the underlying cost function to be minimized has proved to be multi-modal and non-differentiable. Flame detection results of the proposed algorithm are promising.

6. ACKNOWLEDGEMENTS

REFERENCES

[1] Fastcom Technology SA, *Method and Device for Detecting Fires Based on Image Analysis*. PCT Pubn.No. WO02/069292, CH-1006, Lausanne, Switzerland, 2002.

[2] B. W. Albers, A. K. Agrawal, "Schlieren analysis of an oscillating gas-jet diffusion," *Combust. flame*, vol. 119, pp. 84–94, 1999.

[3] W. Phillips III, M. Shah, and N. V. Lobo, "Flame recognition in video," *Pattern Recogn. Lett.*, vol. 23, pp. 319–327, 2002.

[4] T. Chen, P. Wu, and Y. Chiou, "An early fire-detection method based on image processing," in *Proc. ICIP 2004*, 2004, pp. 1707–1710.

[5] B. U. Toreyin, Y. Dedeoglu, U. Gudukbay, and A. E. Cetin, "Computer vision based system for real-time fire and flame detection," *Pattern Recogn. Lett.*, vol. 27, pp. 49–58, 2006.

[6] B. U. Toreyin, Y. Dedeoglu, A. E. Cetin, "HMM Based Falling Person Detection Using Both Audio and Video," in *Proc. IEEE Int. Workshop on Human-Computer Interaction*, Beijing, China, 2005, pp. 211–220.

[7] F. Jabloun, A. E. Cetin, "The Teager energy based feature parameters for robust speech recognition in car noise," in *Proc. IEEE ICASSP'99*, 1999, pp. 273–276.

[8] H. Bunke and T. Caelli, *HMMs Applications in Computer Vision*. World Scientific, 2001.

[9] L.R.Rabiner, B.-H.Juang, *Fundamentals of Speech Recognition*. New Jersey: Prentice-Hall Inc., 1993.

[10] E. Erzin, A. Cetin, and Y. Yardimci, "Subband analysis for robust speech recognition in the presence of car noise," in *Proc. IEEE ICASSP'95*, 1995.

[11] R. Sarikaya, B. L. Pellom, and J. H. Hansen, "Wavelet Packet Transform Features with Application to Speaker Identification," in *Proc. NORSIG '98*, 1998.

[12] R. Sarikaya and J. N. Gowdy, "Subband Based Classification of Speech Under Stress," in *Proc. IEEE ICASSP'98*, 1998, pp. 596–572.

[13] C. W. Kim, R. Ansari, A. E. Cetin, "A class of linear-phase regular biorthogonal wavelets," in *Proc. IEEE ICASSP'92*, 1992, pp. 673–676.

[14] M. Thuillard, "A new flame detector using the latest research on flames and fuzzy-wavelet algorithms," *Fire Safety Journal*, vol. 37, pp. 371–380, 2002.

[15] F. C. Carter, and N. Cross, "Combustion monitoring using infrared array-based detectors," *Measurement Science and Technology*, vol. 14, pp. 1117–1122, 2003.